



18 **Abstract:** Sedimentary records of lipid biomarkers such as leaf wax *n*-alkanes are not only  
19 influenced by ecosystem turnover and physiological changes in plants, they are also influenced by  
20 earth surface processes integrating these signals into the sedimentary record, though the effect of  
21 these integration processes are not fully understood. To determine the depositional constraints on  
22 biomarker records in a high-altitude small catchment system, we collected both soil and stream  
23 sediments along a 1000 m altitude transect (1500 – 2500 masl) in the Areguni Mountains, a  
24 subrange of the Lesser Caucasus Mountains in Armenia. We utilize a treeline at ~ 2000 masl,  
25 which separates alpine meadow above from deciduous forest below, to assess the relative  
26 contribution of upstream biomarker transport to local vegetation input in the stream. We find that  
27 average chain length (ACL), hydrogen isotope ( $\delta D$ ) and carbon isotope ( $\delta^{13}C$ ) values of *n*-alkanes  
28 are significantly different in soils collected above and below the treeline. However, samples  
29 collected from the stream sediments do not integrate these signals quantitatively. As the stream drops  
30 below the treeline, the ACL,  $\delta D$  and  $\delta^{13}C$  values of *n*-alkanes preserved in streambed sediments  
31 reflect a bias toward *n*-alkanes sourced from trees. This suggests that there is either 1) minimal  
32 transportation of organic matter from the more open vegetation in higher elevations, or 2) greater  
33 production of target biomarkers by trees and shrubs found at lower elevations results in  
34 overprinting of stream signals by local vegetation. Though these observations may preclude using  
35 *n*-alkanes to measure past treeline movement in these mountains,  $\delta D$  values of biomarkers in  
36 fluvial deposits in these settings are more likely to record local hydrological changes rather than  
37 reflect fractionation changes due to turnover in upstream vegetation structure.

38

## 39 **1. Introduction**

40 Mountain regions are important hubs for biodiversity and can provide refuge for a number  
41 of endemic species of flora and fauna (Antonelli et al., 2018). However, these high-altitude  
42 environments are often particularly vulnerable to climate change (Guisan and Theurillat, 2000).  
43 Therefore, gaining an understanding of sensitivity of these regions to past climate change is  
44 important for projecting the effects of future climate change on fragile ecosystems. The Caucasus  
45 Region in particular has been identified as a biodiversity hotspot covering the Republics of  
46 Armenia, Georgia, Azerbaijan, and parts of the Russian Federation, Türkiye, and Iran, that  
47 supports a wide variety of plant and animal species (Zazanashvili, 2009; Gasparyan and  
48 Glauberman, 2022). To better understand climate and environmental change in both the past and  
49 the present, it is necessary to refine our understanding and interpretation of paleoclimate records  
50 in this region. Plant wax biomarkers have been used in this region in both geological and  
51 archaeological contexts to reconstruct past climates, therefore understanding modern variability  
52 and transport processes will help refine these interpretations (Brittingham et al., 2019; Glauberman  
53 et al., 2020; Malinsky-Buller et al., 2021, 2024; Trigui et al., 2019). Specifically, we are interested  
54 in understanding the sedimentary processes involved in the formation, transport, recycling, and  
55 accumulation of organic biomarkers in sedimentary archives and assessing whether these archives  
56 record a local environmental signal or are a mix of local and transported organic material.

57 Normal alkanes (*n*-alkanes) are an important component of the epicuticular wax in  
58 terrestrial plants. This waxy coating on plants protects against ultraviolet damage, water loss and  
59 predation (Jetter et al., 2006). Specific compounds in this wax, such as *n*-alkanes, are a useful tool  
60 for reconstructing past environmental changes through the analysis of the distribution of alkane  
61 homologues as well as their stable hydrogen ( $\delta D$ ) and carbon ( $\delta^{13}C$ ) isotope values. Previous

62 research in the Greater and Lesser Caucasus Mountains has documented the applicability of the  
63 average chain length (ACL) of leaf wax biomarkers as a tool for differentiating between grassy  
64 and deciduous vegetation (Bliedtner et al., 2018; Trigui et al., 2019a), although on a global scale  
65 ACL does not differentiate well between vegetation types (Bush and McInerney, 2013a).

66 The carbon isotope ( $\delta^{13}\text{C}$ ) values of plant tissue is primarily determined by the  
67 photosynthetic pathway of the plant (Diefendorf and Freimuth, 2017).  $\text{C}_3$  plants, which thrive in  
68 areas with cooler growing season temperatures, have more negative  $\delta^{13}\text{C}$  values than do  $\text{C}_4$  plants,  
69 which thrive in warmer growing season temperatures (Ehleringer et al., 1977).  $\text{C}_3$  vegetation is  
70 further influenced by water use efficiency, as water stress influences the  $c_i/c_a$  ratio of plants  
71 (Farquhar et al., 1982).  $\delta^{13}\text{C}$  values in lipids generally follow the same trends, and  $\text{C}_3$  plants have  
72 more negative  $\delta^{13}\text{C}$  lipid values than  $\text{C}_4$  plants (Diefendorf and Freimuth, 2017). However, carbon  
73 fractionation of lipids is not consistent in different classes of plants (Diefendorf et al., 2011;  
74 Pedentchouk et al., 2008; Sikes et al., 2013). Currently,  $\text{C}_4$  vegetation makes up around 3% of  
75 plant species in Armenia (Rudov et al., 2020), and was present in the Kalavan region during the  
76 Holocene (Tornero et al., 2016).

77 The hydrogen isotope ( $\delta\text{D}$ ) values of *n*-alkanes in terrestrial plants record the  $\delta\text{D}$  values of  
78 environmental water (Sachse et al., 2012). This is typically reflective of  $\delta\text{D}$  values in precipitation,  
79 though precipitation  $\delta\text{D}$  values can also undergo positive shifts due to soil evaporation. The  $\delta\text{D}$   
80 values of plant waxes are also influenced by fractionation during biological synthesis of lipids,  
81 which imparts a strong negative fractionation on  $\delta\text{D}$  values, as well as transpiration of leaf water  
82 (Gamarra et al., 2016). The fractionation between meteoric water and lipids is typically larger in  
83 gymnosperms than in angiosperms (Oakes and Hren, 2016; Pedentchouk et al., 2008).

84           Despite the benefits in measuring  $\delta D$  and  $\delta^{13}C$  values in *n*-alkanes for understanding  
85 environmental and hydrological processes, not all the processes modifying isotope values from  
86 plant to *n*-alkane deposition are well understood. Sedimentary integration is one of the most poorly  
87 understood aspects of this process (Sachse et al., 2012). A number of studies on the integration of  
88 leaf waxes in catchments have been published in recent years which help clarify these processes  
89 (Alewell et al., 2016; Feakins et al., 2018; Häggi et al., 2016; Hemingway et al., 2016; Ponton et  
90 al., 2014; Suh et al., 2019). Previous studies on the integration of organic biomarkers have  
91 produced mix results, with some demonstrating spatial integration of catchment signals (Alewell  
92 et al., 2016; Feakins et al., 2018; Hemingway et al., 2016), whereas others did not observe this  
93 (Häggi et al., 2016; Ponton et al., 2014). However, these previous studies typically focused on very  
94 large river systems, which will undergo different transport processes than the first-order streams  
95 analyzed in this study. A number of these studies (Alewell et al., 2016; Feakins et al., 2018;  
96 Hemingway et al., 2016; Ponton et al., 2014) also observed seasonal differences in biomarker load  
97 in river sediments.

98           Thus, the sedimentary processes involved in the formation, transport, recycling, and  
99 accumulation of organic biomarkers in first and second order streams are not well understood. One  
100 challenge in assessing these processes in small streams is that the environment and plant  
101 communities are often homogenous, and thus it is not possible to differentiate between local and  
102 upstream transported organic material. To better understand transport processes affecting organic  
103 material in small catchments, we studied a set of streams in the Dany River, a tributary of the  
104 Barepat River, located in the Areguni Mountains in the Lesser Caucasus Range. This stream  
105 system is divided into two distinct ecological regions by the treeline (at ~ 2000 masl), which  
106 separates alpine meadow above the tree line (2000 – 2500 masl) from deciduous forest below

107 (1500 – 2000 masl). To evaluate the input of *n*-alkanes from upstream transported organic material  
108 relative to vegetation near the stream, we collected soil samples on the slopes of the mountains  
109 from both above- and below the treeline throughout the watershed and sediments deposited in the  
110 streambed along an elevation transect. Comparison of the hillside and streambed sedimentary *n*-  
111 alkanes allows assessment of the input of *n*-alkanes locally produced by vegetation compared to  
112 those transported in stream sediments within the catchment.

113 An additional motivation of this research is that treelines are a vulnerable feature of higher  
114 altitude environments. Previous research in the Areguni Mountains study area has assessed the  
115 relationship between treeline dynamics and climate forcing in the past (Ghukasyan et al., 2010;  
116 Malinsky-Buller et al., 2021; Montoya et al., 2013; Tornero et al., 2016). Pleistocene sediments  
117 uncovered at archaeological sites at Kalavan village within this area have the potential to  
118 reconstruct this relationship through the analysis of plant wax biomarkers deposited in fluvial  
119 sediments. However, in order to reconstruct these systems in the past it is important to understand  
120 modern biomarkers integration processes in the first and second order streams and their potential  
121 effects on the sedimentary archives of the Areguni Mountains.

## 122 **2. Methods**

### 123 **2.1 Sample Collection and Extraction**

124 Hillslope soil samples were collected in September 2018 along an altitude transect (1500 – 2500  
125 masl) above the Dany River watershed, a first order tributary of the Barepat River in the Areguni  
126 Mountains, Armenia (Fig 1), which traverses the treeline at ~2000 masl. Forest vegetation is  
127 predominantly oak (*Quercus macranthera*), beech (*Fagus orientalis*) and hornbeam (*Carpinus*  
128 *orientalis*), while above treeline alpine meadow is comprised of *Heracleum sp.* and *Senecio sp.*  
129 (Joannin et al., 2022; Volodicheva, 2002). Soil samples were collected by first clearing the top ~10

130 cm of soil to remove roots. Stream bed sediment samples were collected from the Dany River  
 131 throughout the altitude transect at intervals of ~100 m in altitude. In all cases, roughly 100 g of  
 132 sediment were collected for extraction of *n*-alkanes. Samples were extracted using a Soxhlet  
 133 apparatus with 2:1 dichloromethane:methanol for 48 hours. Following lipid extraction, *n*-alkanes  
 134 were separated from total liquid extract by passing samples through a column of activated silica  
 135 gel (1.25 g) in baked Pasteur pipettes with 2 mL hexane (non-polar fraction), 4 mL  
 136 dichloromethane (slightly polar fraction) and 4 mL methanol (polar fraction). *n*-alkanes were  
 137 quantified through the analysis of the hexane fraction. We quantified *n*-alkanes using a BP-5  
 138 column (30 m × 0.25 mm i.d., 0.25 μm film thickness) with He as the carrier (1.5 ml/min). Oven  
 139 temperature was set at 50 °C for 1 min, ramped to 180 °C at 12 °C/min, then ramped to 320 °C at  
 140 6 °C/min and held for 4 min. (Brittingham et al., 2017; Smolen and Hren, 2023). We measured a  
 141 standard mixture of *n*-alkanes (C<sub>20</sub>-C<sub>33</sub>) of known concentration to correct for mass dependent  
 142 response decreases in longer chain *n*-alkanes. Odd over even predominance (OEP) (Eq. 1) and  
 143 average chain length (ACL) (Eq. 2) were used to evaluate distributions of *n*-alkanes (Bush and  
 144 McInerney, 2013b). We also calculated P<sub>aq</sub>, an *n*-alkane proxy to evaluate the possible biomarker  
 145 contribution of aquatic and emergent plants (Eq. 3) (Ficken et al., 2000).

$$146 \quad \text{OEP} = \frac{C_{25} + C_{27} + C_{29} + C_{31} + C_{33}}{C_{24} + C_{26} + C_{28} + C_{30} + C_{32}}$$

$$147 \quad \text{ACL} = \frac{25 * C_{25} + 27 * C_{27} + 29 * C_{29} + 31 * C_{31} + 33 * C_{33}}{C_{25} + C_{27} + C_{29} + C_{31} + C_{33}}$$

$$148 \quad \text{P}_{\text{aq}} = \frac{C_{23} + C_{25}}{C_{23} + C_{25} + C_{29} + C_{31}}$$

### 149 **2.3 Stable Isotope Analysis**

150  $\delta\text{D}$  and  $\delta^{13}\text{C}$  values of individual *n*-alkanes were measured with a Thermo GC-Isolink coupled  
151 with a Thermo Scientific MAT 253 (manufacturer) isotope ratio mass spectrometer with a BP-5  
152 column (30 m  $\times$  0.25 mm i.d., 0.25  $\mu\text{m}$  film thickness). Oven temperature was set at 50°C for 1  
153 min, ramped to 180°C at 12°C/min, then ramped to 320°C at 6°C/min and held for 4 min. Internal  
154 standards (Mix A5 from A. Schimmelman) were run every four samples across a range of  
155 concentrations (5-30 V/s) to correct for size effects. Standard errors were 0.4‰ for  $\delta^{13}\text{C}$  and 3‰  
156 for  $\delta\text{D}$ . Isotope ratios (R) were converted to  $\delta\text{X}$  ( $\delta^{13}\text{C}$  and  $\delta\text{D}$ ) values (Eq. 3) and are expressed in  
157 permill (‰).

$$158 \quad \delta\text{X} = \left( \frac{R_{\text{Sample}}}{R_{\text{Standard}}} - 1 \right) * 1000$$

159

### 160 **3. Results**

#### 161 **3.1. Alkane abundances**

162 The most abundant alkane homolog in samples collected in the Areguni Mountains is the  
163  $\text{C}_{29}$  or  $\text{C}_{31}$  alkane, which is typical for terrestrial plants (see S1-S4 for illustrative chromatograms).  
164 Odd numbered alkanes are significantly more abundant than even numbered alkanes, and the OEP  
165 of all samples is 11.2, with a range from 7.4-18.4. There is no significant difference between the  
166 mean OEP of soil (11.1) and stream (11.3) samples in the watershed. These values are similar to  
167 those previously measured in the Greater and Lesser Caucasus Mountains (Bliedtner et al., 2018;  
168 Trigui et al., 2019).

169 The mean average chain length (ACL) of all samples averages 29.7, with a range from 28.4  
170 to 31.8 (Fig 3). In soils above the treeline, the mean ACL value is 30.6 (range of 29.8-31.8). In  
171 soils below the treeline, the mean ACL value is 29.5 (range of 28.4-30.4). There is a significant



172 difference between the average ACL values of the *n*-alkanes in above treeline and below treeline  
173 soils (Student's t-test,  $p < 0.001$ ,  $n = 30$ ). Stream sediment above the treeline have an average ACL  
174 value of 29.7 (range of 29.1-30.2) and stream sediments below the treeline have an average ACL  
175 value of 29.3 (range of 28.6 -30.0). The stream sediments from below the treeline have a  
176 significantly (Student's t-test,  $p < 0.001$ ,  $n = 21$ ) lower average ACL value than those above the  
177 treeline.

178 The  $P_{aq}$  values of *n*-alkanes in these samples suggests a mostly terrestrial origin of the  
179 organic matter. Higher  $P_{aq}$  values indicate contributions of floating and emergent macrophytes.  
180 However, we do not find a difference between the  $P_{aq}$  values in the stream sediments when  
181 compared to the soil samples, indicating that the organic load of the stream sediments is mostly of  
182 terrestrial origin. Terrestrial plants have average  $P_{aq}$  values of 0.09, with emergent plants averaging  
183 0.25 (Ficken et al., 2000). Only eight of the 51 samples in this study had  $P_{aq}$  values above 0.20,  
184 four stream and four soil samples. This indicates that there was not a significant contribution of  
185 aquatic plants in the Dany stream sediments, and the biomarker load is primarily terrestrial in  
186 origin.

### 187 **3.2. $\delta D$ and $\delta^{13}C$ values**

188 The  $\delta^{13}C$  values in soils and stream sediments collected from the Areguni Mountains reflect  
189 a  $C_3$  landscape, which is typical in Armenia.  $\delta^{13}C$  values in all samples ranged from -36.0 to -  
190 32.3‰ (Fig 4). The range is similar for both soil samples (-35.9 to -32.3‰) and stream samples (-  
191 36.0 to -32.5‰). However, there is a significant difference in the  $\delta^{13}C$  values of above and below  
192 treeline samples, both in the stream and soil samples collected. Above the treeline,  $\delta^{13}C$  values in  
193 soils average -34.9‰, and below the treeline soil alkanes average -33.3‰ ( $p < 0.0001$ , student's t-  
194 test,  $n = 30$ ). Stream sediment  $\delta^{13}C$  values average -35.0‰ above the treeline and -33.6‰ below

195 the treeline ( $p < 0.0001$ , student's t-test,  $n=21$ ).  $\delta^{13}\text{C}$  values in stream samples exhibit a step-like  
196 behavior, with  $\sim 2\text{‰}$  shift to more negative values as the stream drops below the treeline.

197 The  $\delta\text{D}$  values measured in soil samples collected in the catchment ranged from  $-144$  to -  
198  $185\text{‰}$  (Fig 5). These values were significantly more negative in above treeline sediments ( $-175\text{‰}$ )  
199 than in below treeline sediments ( $-156\text{‰}$ ) ( $p < 0.001$ , student's t-test,  $n=30$ ).  $\delta\text{D}$  values were also  
200 more negative in stream sediment samples collected above the treeline ( $-175\text{‰}$ ) than below the  
201 treeline ( $-158\text{‰}$ ) ( $p < 0.001$ , student's t-test,  $n=21$ ). As with the  $\delta^{13}\text{C}$  values, the  $\delta\text{D}$  values of  
202 stream sediment samples show sudden change as the stream drops below the treeline.

## 203 **4. Discussion**

### 204 **4.1 Integration of local and upstream soil *n*-alkanes into the river sediments**

205 The hillslope soil leaf wax ACL (Fig 3),  $\delta^{13}\text{C}$  (Fig. 4) and  $\delta\text{D}$  (Fig. 5) show a step-like  
206 change at the treeline, indicating a significant separation between upstream (above treeline) and  
207 downstream (below treeline) soils. Using this separation, it is possible to assess the contributions  
208 and integration of upstream vs. downstream soils to the streambed sediments along the altitude  
209 transect. The step-like transition in streambed  $\delta\text{D}$  and  $\delta^{13}\text{C}$  values indicates an over-printing of  
210 upstream alkane isotope values by input from deciduous vegetation. Thus, local production largely  
211 outweighs upstream transport in this setting. However, to firmly evaluate the upstream and  
212 downstream hillslope soil contribution to streambed sediments, there is a need to quantitatively  
213 evaluate the area-weighted production of *n*-alkanes above and below the treeline.

### 214 **4.2. Modeling *n*-alkane production and estimating upstream transport and integration**

215 To further evaluate the integration of *n*-alkanes above and below the treeline, we created a  
216 mixing model that calculates the expected  $\delta\text{D}$ ,  $\delta^{13}\text{C}$  and ACL values at each one of the sampling  
217 locations based on the *n*-alkane production of hillslope sediments above each streambed sampling

218 point (Fig. 6). Our mixing model assumes that the *n*-alkanes in the river are a function of the  
219 weighted *n*-alkane production above the sampling location.

220 The parameters we used for our mixing model are: 1. Satellite images (Google Earth) to  
221 map the areas covered by alpine meadow and forest vegetation throughout the Dany River  
222 catchment. 2. An estimate of net primary productivity of organic material production in grasses  
223 and trees (grams per area) (Brun et al., 2022). 3. Estimates of *n*-alkane production in grasses and  
224 trees in the Greater and Lesser Caucasus Mountains (grams of *n*-alkane per gram of organic  
225 material) (Bliedtner et al., 2018; Trigui et al., 2019). 4. End member values of  $\delta D$ ,  $\delta^{13}C$  and ACL  
226 derived from the average hillslope soils above and below the treeline. At each sample point within  
227 the catchment, we first calculated the upstream area covered by the two dominant vegetation types  
228 within the catchment (deciduous forest and alpine meadow) (Figure 6). This area was then  
229 multiplied by the previously mentioned constants (Table 1). By multiplying these terms (area x  
230 organic mass production x *n*-alkane production x end member soils value), we created an *n*-alkane  
231 production map for the Dany River catchment. Using this method, we calculated, the amount of  
232 grass and tree *n*-alkanes produced on the hillslopes above the sampling locations and the expected  
233  $\delta D$ ,  $\delta^{13}C$  and ACL values for each stream sampling location (Figure 7a, 7c, 7e).

234 We compared the results of our mixing model with the measured  $\delta D$ ,  $\delta^{13}C$  and ACL in the  
235 streams. Stream sediment samples collected above the treeline (from ~2000-2600 masl) fall within  
236 the range of expected values, however, samples below the treeline consistently over-sample *n*-  
237 alkanes sourced from below treeline vegetation. Measured  $\delta D$ ,  $\delta^{13}C$  and ACL values do not have  
238 a linear relationship with the expected values based on vegetation area (Fig 7b, 7d, 7f). These  
239 measured values would produce under-estimates of the upstream area of alpine grasses, yielding  
240 incorrect reconstructions of paleo-vegetation in sedimentary records. Comparing the mixing model

241 with the observations indicates that an area-weighted mixing process is not an adequate model for  
242 explaining the *n*-alkanes signal in the streambed sediments. A simple and straightforward way to  
243 interpret this discrepancy is that an area-weighted quantitative integration of *n*-alkanes is not a  
244 good model for describing this catchment system, and that local production is much larger than  
245 transported organic material.

246         However, there are still other factors that may be driving this process that our mixing model  
247 does not account for. First, the average slope of forested areas in the Dany watershed is higher than  
248 those in grassy areas. These steeper slopes would cause more sediment transport into the stream  
249 bed. Second, although production of *n*-alkanes in grasses and trees is not significantly different in  
250 the Greater and Lesser Caucasus Mountains, concentrations are higher in soils in deciduous areas  
251 (Bliedtner et al., 2018; Trigui et al., 2019). This retention of more biomarkers in forest soils would  
252 also increase the contribution of deciduous alkanes into the stream bed. Third, stream downcutting  
253 into older sediments has the potential to re-mobilize stored organic carbon, which may contain a  
254 greater load of deciduous *n*-alkanes. However, analysis of pollen from a lake core nearby (~ 5km  
255 from the Dany catchment) in the Areguni Mountains shows a gradual shift over the last 4000 years  
256 from a grass-dominated landscape to the deciduous forest present today (Joannin et al., 2022b).  
257 Therefore, stored biomarkers are more likely to be grass-dominant, and this is unlikely to explain  
258 the measured bias to deciduous alkanes.

259         Since *n*-alkanes in the first order stream in this study do not quantitatively integrate *n*-alkanes  
260 based on the upstream area of different vegetation types, this likely precludes the use of *n*-alkanes  
261 as a tool to reconstruct vertical treeline movement in this setting. However, this is a benefit for  
262 attempts to reconstruct hydrological changes through the analysis of  $\delta D$  values in *n*-alkanes. Given  
263 the ~20‰ difference in apparent fractionation ( $\epsilon$ ) values for above and below treeline sediments,

264 changes in upstream vegetation cover would alter measured  $\delta D$  values in *n*-alkanes in sedimentary  
265 archives. Without this quantitative integration, *n*-alkanes measured in the Pleistocene sediments  
266 found in this watershed are more likely to reflect changes in  $\delta D$  values of precipitation, and  
267 therefore would serve to reconstruct hydrological cycles, rather than changes in upstream  
268 vegetation cover. Since  $\delta^{13}C$  and ACL of *n*-alkanes are also different in above and below treeline  
269 sediments, these other analyses would also be useful to identify periods with large changes in  
270 treeline that might complicate interpretation of  $\delta D$  values.

271 In order to illustrate this point, we present hypothetical records of biomarker  $\delta D$  values  
272 from three points in the Dany watershed (Fig. 7) documenting 20‰ and 30‰ shifts in precipitation  
273  $\delta D$  values. We use  $\delta D$  values of precipitation from water samples collected at the nearest  
274 meteorological station with isotope data in Armenia (Dilijan, Brittingham et al., 2019b) Given the  
275 lack of quantitative integration in the catchment, a paleoclimate record from either above (A) or  
276 below (C) treeline would record the shift in precipitation  $\delta D$  values. Below treeline sedimentary  
277 records, with stream organic biomarker load overprinted by local vegetation production, would  
278 likely provide a means to reconstruct the  $\delta D$  precipitation values. However, records near the  
279 treeline (B) would be influenced by changes in apparent fractionation values associated with  
280 changes in vegetation around the stream. Co-occurring climate forcing of shifts in  $\delta D$  values of  
281 precipitation and changes in treeline altitude would cause paleoclimate records in this zone to over-  
282 estimate the magnitude of precipitation  $\delta D$  value shifts.

283

## 284 **5. Conclusion**

285 Sediment and stream samples from the Areguni Mountains, a subrange of the Lesser Caucasus  
286 Mountains in Armenia, demonstrate that there is a significant difference in hillslope soil  $\delta D$ ,  $\delta^{13}C$

287 and ACL values above and below treeline. *n*-alkanes in sediments in the Areguni Mountains can  
288 be used to differentiate between the above and below treeline sediments. However, *n*-alkanes  
289 extracted from stream sediments reflect their local area, rather than demonstrating transport from  
290 the higher-altitude alpine meadow. These results provide a complication for attempts to reconstruct  
291 changes in past treeline in this mountain range, given that the biomarker load in stream does not  
292 reflect the relative area of different upstream vegetation types. However, these results simplify  
293 interpretation of past *n*-alkane  $\delta D$  values, as apparent fractionation differences between grasses  
294 and trees are less likely to impart a significant influence on  $\delta D$  values in stream bed *n*-alkanes.

## 295 **6. Competing interests**

296 The contact author has declared that none of the authors has any competing interests

## 297 **7. Acknowledgements**

298 We would like to thank the Kalavan villagers for their help, support, and hospitality: especially  
299 the Ghukasyan family for providing us a home away from home. We also thank Suren Kesejyan,  
300 Hovhannes Partevyan, and Vardan Stepanyan. The research in Kalavan project was funded by the  
301 support of The Gerda Henkel Stiftung grant n. AZ 10\_V\_17 and n. AZ 23/F/19, the Leakey  
302 Foundation. AB is thankful to the Lady Davis foundation, Fritz-Thyssen Foundation grant awarded  
303 for the project “Pleistocene Hunter-Gatherer Lifeways and Population Dynamics in the Ararat  
304 (paleo-lake) Depression, Armenia”, and The European Research Council grant N 948015:  
305 “Investigating Pleistocene population dynamics in the Southern Caucasus” (awarded to AMB) for  
306 current financial support. Further support was provided by “Areni-1 Cave” Consortium [“Areni-1  
307 Cave” Scientific-Research Foundation (Armenia), and the “Gfoeller Renaissance Foundation”  
308 (USA)], as well as the Institute of Archaeology and Ethnography of the National Academy of  
309 Sciences of the Republic of Armenia (supported by the Higher Education and Science Committee,

310 Republic of Armenia, under grant number 21AG-6A080). We would like to thank Joseph Novak  
311 and an anonymous reviewer for their helpful comments on the manuscript.

312

313 **References**

314

315 Alewell, C., Birkholz, A., Meusburger, K., Schindler Wildhaber, Y., and Mabit, L.: Quantitative  
316 sediment source attribution with compound-specific isotope analysis in a C3 plant-  
317 dominated catchment (central Switzerland), *Biogeosciences*, 13, 1587–1596,  
318 <https://doi.org/10.5194/bg-13-1587-2016>, 2016.

319

320 Antonelli, A., Kissling, W. D., Flantua, S. G. A., Bermúdez, M. A., Mulch, A., Muellner-Riehl,  
321 A. N., Kreft, H., Linder, H. P., Badgley, C., Fjeldså, J., Fritz, S. A., Rahbek, C., Herman,  
322 F., Hooghiemstra, H., and Hoorn, C.: Geological and climatic influences on mountain  
323 biodiversity, *Nat Geosci*, 11, 718–725, <https://doi.org/10.1038/s41561-018-0236-z>, 2018.

324

325 Bliedtner, M., Schäfer, I. K., Zech, R., and Von Suchodoletz, H.: Leaf wax n-alkanes in modern  
326 plants and topsoils from eastern Georgia (Caucasus) - Implications for reconstructing  
327 regional paleovegetation, *Biogeosciences*, 15, 3927–3936, [https://doi.org/10.5194/bg-15-](https://doi.org/10.5194/bg-15-3927-2018)  
328 [3927-2018](https://doi.org/10.5194/bg-15-3927-2018), 2018.

329

330 Brittingham, A., Hren, M., and Hartman, G.: Microbial alteration of the hydrogen and carbon  
331 isotopic composition of n-alkanes in sediments, *Org Geochem*, 107, 1–8,  
332 <https://doi.org/10.1016/j.orggeochem.2017.01.010>, 2017.

333

334 Brittingham, A., Hren, M. T., Hartman, G., Wilkinson, K. N., Mallol, C., Gasparyan, B., and  
335 Adler, D. S.: Geochemical Evidence for the Control of Fire by Middle Palaeolithic  
336 Hominins, *Sci Rep*, 9, <https://doi.org/10.1038/s41598-019-51433-0>, 2019a.

337

338 Brittingham, A., Petrosyan, Z., Hepburn, J. C., Richards, M. P., Hren, M. T., and Hartman, G.:  
339 Influence of the North Atlantic Oscillation on  $\delta D$  and  $\delta^{18}O$  in meteoric water in the  
340 Armenian Highland, *J Hydrol (Amst)*, 575, 513–522,  
341 <https://doi.org/10.1016/j.jhydrol.2019.05.064>, 2019b.

342

343 Brun, P., Zimmermann, N. E., Hari, C., Pellissier, L., and Karger, D. N.: Global climate-related  
344 predictors at kilometer resolution for the past and future, *Earth Syst Sci Data*, 14, 5573–  
345 5603, <https://doi.org/10.5194/essd-14-5573-2022>, 2022.

346

347 Bush, R. T. and McInerney, F. A.: Leaf wax n-alkane distributions in and across modern plants:  
348 Implications for paleoecology and chemotaxonomy, *Geochim Cosmochim Acta*, 117,  
349 161–179, <https://doi.org/10.1016/j.gca.2013.04.016>, 2013.

350

351



352 Diefendorf, A. F. and Freimuth, E. J.: Extracting the most from terrestrial plant-derived n-alkyl  
353 lipids and their carbon isotopes from the sedimentary record: A review, *Org Geochem*,  
354 103, 1–21, <https://doi.org/10.1016/j.future.2015.08.005>, 2017.  
355

356 Diefendorf, A. F., Freeman, K. H., Wing, S. L., and Graham, H. V.: Production of n-alkyl lipids  
357 in living plants and implications for the geologic past, *Geochim Cosmochim Acta*, 75,  
358 7472–7485, <https://doi.org/10.1016/j.gca.2011.09.028>, 2011.  
359

360 Ehleringer, J., Björkman, O., and Bjorkman, O.: Quantum yields for CO<sub>2</sub> uptake in C<sub>3</sub> and C<sub>4</sub>  
361 plants, *Plant Physiol*, 59, 86–90, 1977.  
362

363 Farquhar, G. D., O’Leary, M. H., and Berry, J. A.: On the Relationship between Carbon Isotope  
364 Discrimination and the Intercellular Carbon Dioxide Concentration in Leaves, *Aust J*  
365 *Plant Physiol*, 9, 121–137, 1982.  
366

367 Feakins, S. J., Wu, M. S., Ponton, C., Galy, V., and West, A. J.: Dual isotope evidence for  
368 sedimentary integration of plant wax biomarkers across an Andes-Amazon elevation  
369 transect, *Geochim Cosmochim Acta*, 242, 64–81,  
370 <https://doi.org/10.1016/j.gca.2018.09.007>, 2018a.  
371

372 Ficken, K. J., Li, B., Swain, D. L., and Eglinton, G.: An n -alkane proxy for the sedimentary  
373 input of submerged floating freshwater aquatic macrophytes, *Org Geochem*, 31, 745–749,  
374 2000.  
375

376 Gamarra, B., Sachse, D., and Kahmen, A.: Effects of leaf water evaporative 2H-enrichment and  
377 biosynthetic fractionation on leaf wax n-alkane  $\delta^2\text{H}$  values in C<sub>3</sub> and C<sub>4</sub> grasses, *Plant*  
378 *Cell Environ*, 39, 2390–2403, <https://doi.org/10.1111/pce.12789>, 2016.  
379

380 Ghukasyan, R., Colonge, D., Nahapetyan, S., Ollivier, V., Gasparyan, B., Monchot, H., and  
381 Chataigner, C.: Kalavan-2 (North of Lake Sevan, Armenia): A new late middle  
382 paleolithic site in the Lesser Caucasus, *Archaeology, Ethnology and Anthropology of*  
383 *Eurasia*, 38, 39–51, <https://doi.org/10.1016/j.aeae.2011.02.003>, 2010.  
384

385 Glauberman, P., Gasparyan, B., Sherriff, J., Wilkinson, K., Li, B., Knul, M., Brittingham, A.,  
386 Hren, M. T., Arakelyan, D., Nahapetyan, S., Raczynski-henk, Y., Haydosyan, H., and  
387 Adler, D. S.: Barozh 12 : Formation processes of a late Middle Paleolithic open-air site in  
388 western Armenia, *Quat Sci Rev*, 236, 106276, 2020.  
389

390 Guisan, A. and Theurillat, J.-P.: Assessing alpine plant vulnerability to climate change: a  
391 modeling perspective., *Integrated Assessment*, 307–320, 2000.  
392

393 Häggi, C., Sawakuchi, A. O., Chiessi, C. M., Mulitza, S., Mollenhauer, G., Sawakuchi, H. O.,  
394 Baker, P. A., Zabel, M., and Schefuß, E.: Origin, transport and deposition of leaf-wax

395 biomarkers in the Amazon Basin and the adjacent Atlantic, *Geochim Cosmochim Acta*,  
396 192, 149–165, <https://doi.org/10.1016/j.gca.2016.07.002>, 2016a.  
397

398 Hemingway, J. D., Schefuß, E., Dinga, B. J., Pryer, H., and Galy, V. V.: Multiple plant-wax  
399 compounds record differential sources and ecosystem structure in large river catchments,  
400 *Geochim Cosmochim Acta*, 184, 20–40, <https://doi.org/10.1016/j.gca.2016.04.003>, 2016.  
401

402 Jetter, R., Kunst, L., and Samuels, A. L.: Composition of plant cuticular waxes, in: *Biology of*  
403 *the Plant Cuticle*, edited by: Riederer, M. and Miller, C., Blackwell Publishing Ltd,  
404 Oxford, 145–181, 2006.  
405

406 Joannin, S., Capit, A., Ollivier, V., Bellier, O., Brossier, B., Mourier, B., Tozalakian, P.,  
407 Colombié, C., Yevadian, M., Karakhanyan, A., Gasparyan, B., Malinsky-Buller, A.,  
408 Chataigner, C., and Perello, B.: First pollen record from the Late Holocene forest  
409 environment in the Lesser Caucasus, *Rev Palaeobot Palynol*, 304,  
410 <https://doi.org/10.1016/j.revpalbo.2022.104713>, 2022a.  
411

412 Malinsky-Buller, A., Glauberman, P., Ollivier, V., Lauer, T., Timms, R., Frahm, E., Brittingham,  
413 A., Triller, B., Kindler, L., Knul, M. V., Krakovsky, M., Joannin, S., Hren, M. T., Bellier,  
414 O., Clark, A. A., Blockley, S. P. E., Arakelyan, D., Marreiros, J., Paixaco, E., Calandra,  
415 I., Ghukasyan, R., Nora, D., Nir, N., Adigoyalyan, A., Haydosyan, H., and Gasparyan,  
416 B.: Short-Term occupations at high elevation during the Middle Paleolithic at Kalavan 2  
417 (Republic of Armenia), *PLoS One*, 16, <https://doi.org/10.1371/journal.pone.0245700>,  
418 2021.  
419

420 Malinsky-Buller, A., Edeltin, L., Ollivier, V., Joannin, S., Peyron, O., Lauer, T., Frahm, E.,  
421 Brittingham, A., Hren, M. T., Sirdeys, N., Glauberman, P., Adigoyalyan, A., and  
422 Gasparyan, B.: The environmental and cultural background for the reoccupation of the  
423 Armenian Highlands after the Last Glacial Maximum: The contribution of Kalavan 6, *J*  
424 *Archaeol Sci Rep*, 56, <https://doi.org/10.1016/j.jasrep.2024.104540>, 2024.  
425

426 Montoya, C., Balasescu, A., Joannin, S., Ollivier, V., Liagre, J., Nahapetyan, S., Ghukasyan, R.,  
427 Colonge, D., Gasparyan, B., and Chataigner, C.: The Upper Palaeolithic site of Kalavan 1  
428 (Armenia): An Epigravettian settlement in the Lesser Caucasus, *J Hum Evol*, 65, 621–  
429 640, <https://doi.org/10.1016/j.jhevol.2013.07.011>, 2013.  
430

431 Oakes, A. M. and Hren, M. T.: Temporal variations in the  $\delta D$  of leaf n-alkanes from four riparian  
432 plant species, *Org Geochem*, 97, 122–130,  
433 <https://doi.org/10.1016/j.orggeochem.2016.03.010>, 2016.  
434

435 Pedentchouk, N., Sumner, W., Tipple, B., and Pagani, M.:  $\delta^{13}C$  and  $\delta D$  compositions of n-  
436 alkanes from modern angiosperms and conifers: An experimental set up in central

437 Washington State, USA, *Org Geochem*, 39, 1066–1071,  
438 <https://doi.org/10.1016/j.orggeochem.2008.02.005>, 2008.

439

440 Ponton, C., West, A. J., Feakins, S. J., and Galy, V.: Leaf wax biomarkers in transit record river  
441 catchment composition, *Geophys Res Lett*, 41, 6420–6427,  
442 <https://doi.org/10.1002/2014GL061184>. Received, 2014.

443

444 Rudov, A., Mashkour, M., Djamali, M., and Akhiani, H.: A Review of C4 Plants in Southwest  
445 Asia: An Ecological, Geographical and Taxonomical Analysis of a Region With High  
446 Diversity of C4 Eudicots, *Front Plant Sci*, 11, <https://doi.org/10.3389/fpls.2020.546518>,  
447 2020.

448

449 Sachse, D., Billault, I., Bowen, G. J., Chikaraishi, Y., Dawson, T. E., Feakins, S. J., Freeman, K.  
450 H., Magill, C. R., McInerney, F. a., van der Meer, M. T. J. J., Polissar, P., Robins, R. J.,  
451 Sachs, J. P., Schmidt, H.-L., Sessions, A. L., White, J. W. C., West, J. B., and Kahmen,  
452 A.: Molecular paleohydrology: interpreting the hydrogen-isotopic composition of lipid  
453 biomarkers from photosynthesizing organisms, *Annu Rev Earth Planet Sci*, 40, 221–249,  
454 <https://doi.org/10.1146/annurev-earth-042711-105535>, 2012.

455

456 Sikes, E. L., Medeiros, P. M., Augustinus, P., Wilmshurst, J. M., and Freeman, K. R.: Seasonal  
457 variations in aridity and temperature characterize changing climate during the last  
458 deglaciation in New Zealand, *Quat Sci Rev*, 74, 245–256,  
459 <https://doi.org/10.1016/j.quascirev.2013.01.031>, 2013.

460

461 Smolen, J. D. and Hren, M. T.: Differential effects of clay mineralogy on thermal maturation of  
462 sedimentary n-alkanes, *Chem Geol*, 634, <https://doi.org/10.1016/j.chemgeo.2023.121572>,  
463 2023.

464

465 Suh, Y. J., Diefendorf, A. F., Bowen, G. J., Cotton, J. M., and Ju, S. J.: Plant wax integration and  
466 transport from the Mississippi River Basin to the Gulf of Mexico inferred from GIS-  
467 enabled isoscapes and mixing models, *Geochim Cosmochim Acta*, 257, 131–149,  
468 <https://doi.org/10.1016/j.gca.2019.04.022>, 2019.

469

470 Tornero, C., Balasse, M., Bălăşescu, A., Chataigner, C., Gasparyan, B., and Montoya, C.: The  
471 altitudinal mobility of wild sheep at the Epigravettian site of Kalavan 1 (Lesser Caucasus,  
472 Armenia): Evidence from a sequential isotopic analysis in tooth enamel, *J Hum Evol*, 97,  
473 27–36, <https://doi.org/10.1016/j.jhevol.2016.05.001>, 2016b.

474

475 Trigui, Y., Wolf, D., Sahakyan, L., Hovakimyan, H., Sahakyan, K., Zech, R., Fuchs, M.,  
476 Wolpert, T., Zech, M., and Faust, D.: First calibration and application of leaf wax n-  
477 alkane biomarkers in loess-paleosol sequences and modern plants and soils in Armenia,  
478 *Geosciences (Switzerland)*, 9, <https://doi.org/10.3390/geosciences9060263>, 2019.

479

480

481 Volodicheva, N.: The Caucasus, The physical geography of northern Eurasia, 350–376, 2002.

482

483

484

485

486

487

488

489

490

491

492

	<b>Conc<sup>1</sup></b>	<b>NPP<sup>2</sup></b>	<b>ACL<sup>3</sup></b>	<b><math>\delta^{13}\text{C}^3</math></b>	<b><math>\delta\text{D}^3</math></b>
<b>Forest</b>	7.69	1099.4	29.5	-33.3	-156
<b>Alpine Meadow</b>	3.03	719.1	30.6	-34.9	-175

**Table 1:** Constants used for mixing model. 1: *n*-alkane concentration in grasses and trees in the Caucasus Mountains (grams of *n*-alkane/gram of organic material) (Bliedtner et al., 2018; Trigui et al., 2019). 2: NPP for forest and grassland areas (grams per area) (Brun et al., 2022). 3: mean values for ACL,  $\delta^{13}\text{C}$  and  $\delta\text{D}$  (this study)

494 Figure Captions

495 Figure 1: (Left) Topographic map (ASTER Global DEM) of Armenia with inset map of  
496 sampling location (black box) (Right) Inset map of soil (yellow circles) and stream (blue circles)  
497 samples collected in the Areguni Mountains, along with the limit of the Barepat (dashed line)  
498 and Dany watersheds (solid line)

499 Figure 2: The  $\delta D$  and  $\delta^{13}C$  values of *n*-alkanes extracted from above treeline (green squares) and  
500 below treeline (red triangles) sediments

501 Figure 3: The average chain length (ACL) values of *n*-alkanes extracted from above treeline  
502 (yellow squares) and below treeline (green squares) sediment across the sampling elevation  
503 gradient

504 Figure 4: The  $\delta^{13}C$  values of *n*-alkanes extracted from above treeline (yellow squares) and below  
505 treeline (green squares) sediment across the sampling elevation gradient

506 Figure 5: The  $\delta D$  values of *n*-alkanes extracted from above treeline (yellow squares) and below  
507 treeline (green squares) sediment across the sampling elevation gradient

508 Figure 6: Mixing model used to calculate expected values of stream sample points. Upstream  
509 watershed area covered by deciduous forest (green) and alpine meadow (yellow) was calculated  
510 at each sample location (blue dots). Point watershed for sample 24 (dashed line) is shown here as  
511 an example.

512 Figure 7: Comparison of the measured ACL,  $\delta D$  and  $\delta^{13}C$  values against expected values of  
513 stream sediments. Dashed line represents the range of expected values from stream sediments if  
514 vegetation was integrated equally by area

515 Figure 8: A photograph of the Dany watershed with hypothetical paleoclimate record from three  
516 locations: (A, dashed line) Below treeline, (B, solid line) near treeline with fluctuations in  
517 treeline altitude, and (C, dotted line) above treeline

518

519

520

521

522

523

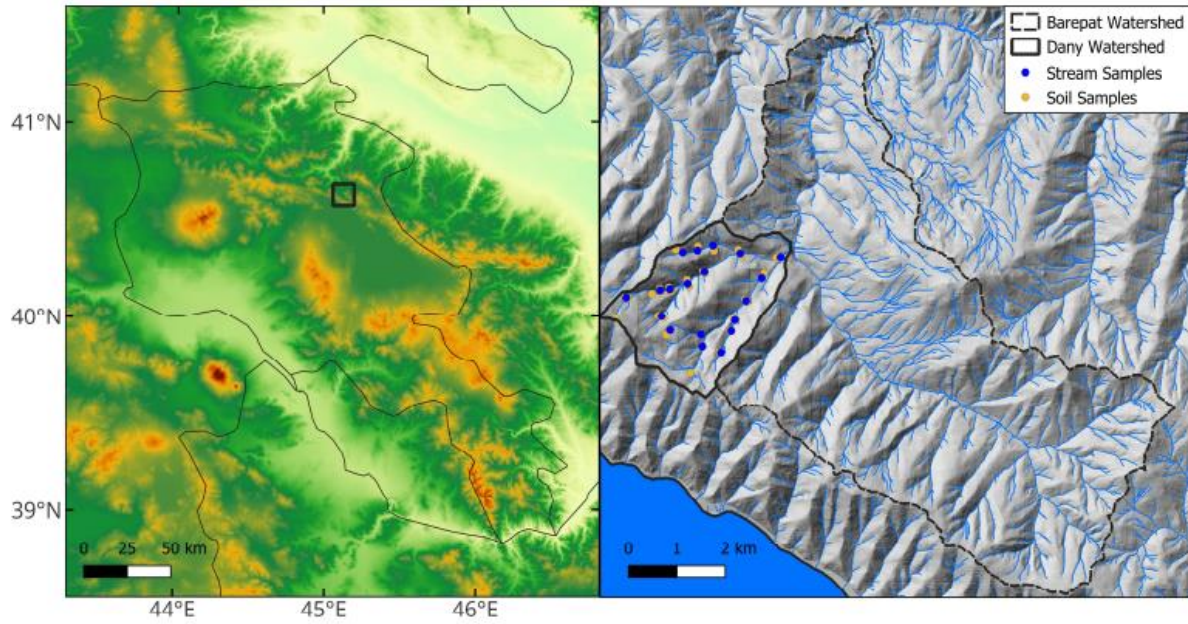


Figure 1: (Left) Topographic map of Armenia with inset map of sampling location (black box) (Right) Inset map of soil (yellow circles) and stream (blue circles) samples collected in the Areguni Mountains, along with the limit of the Barepat (dashed line) and Dany watersheds (solid line)

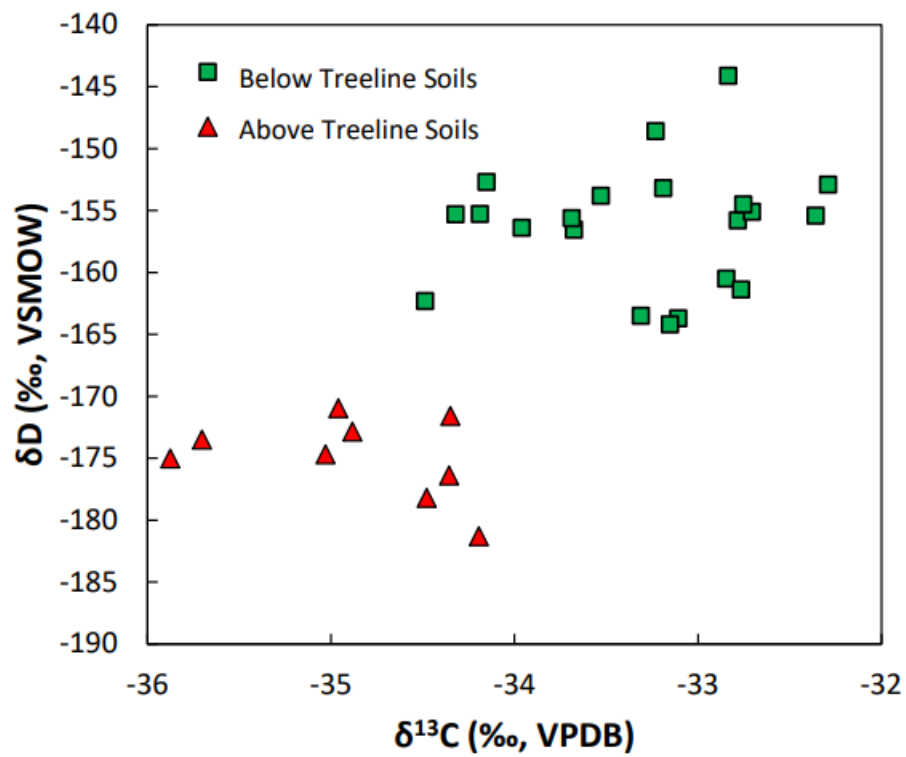
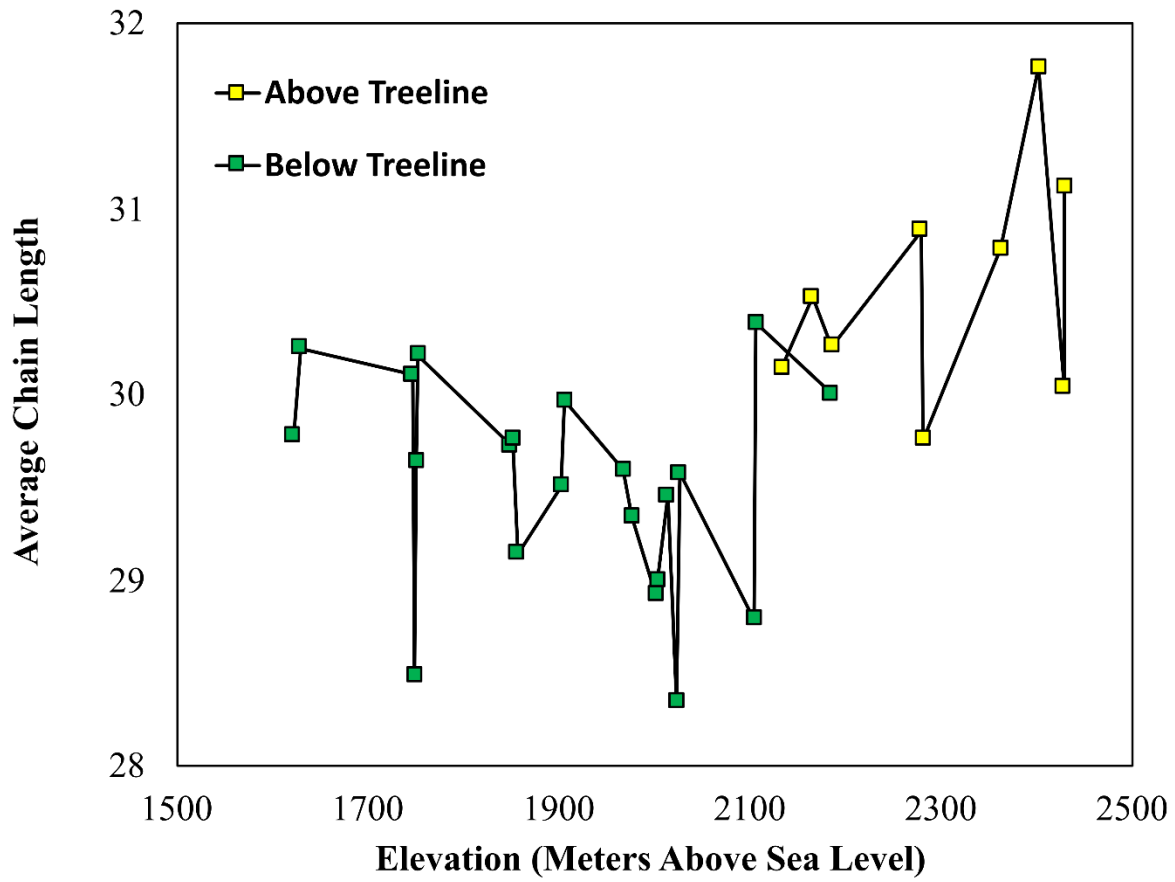


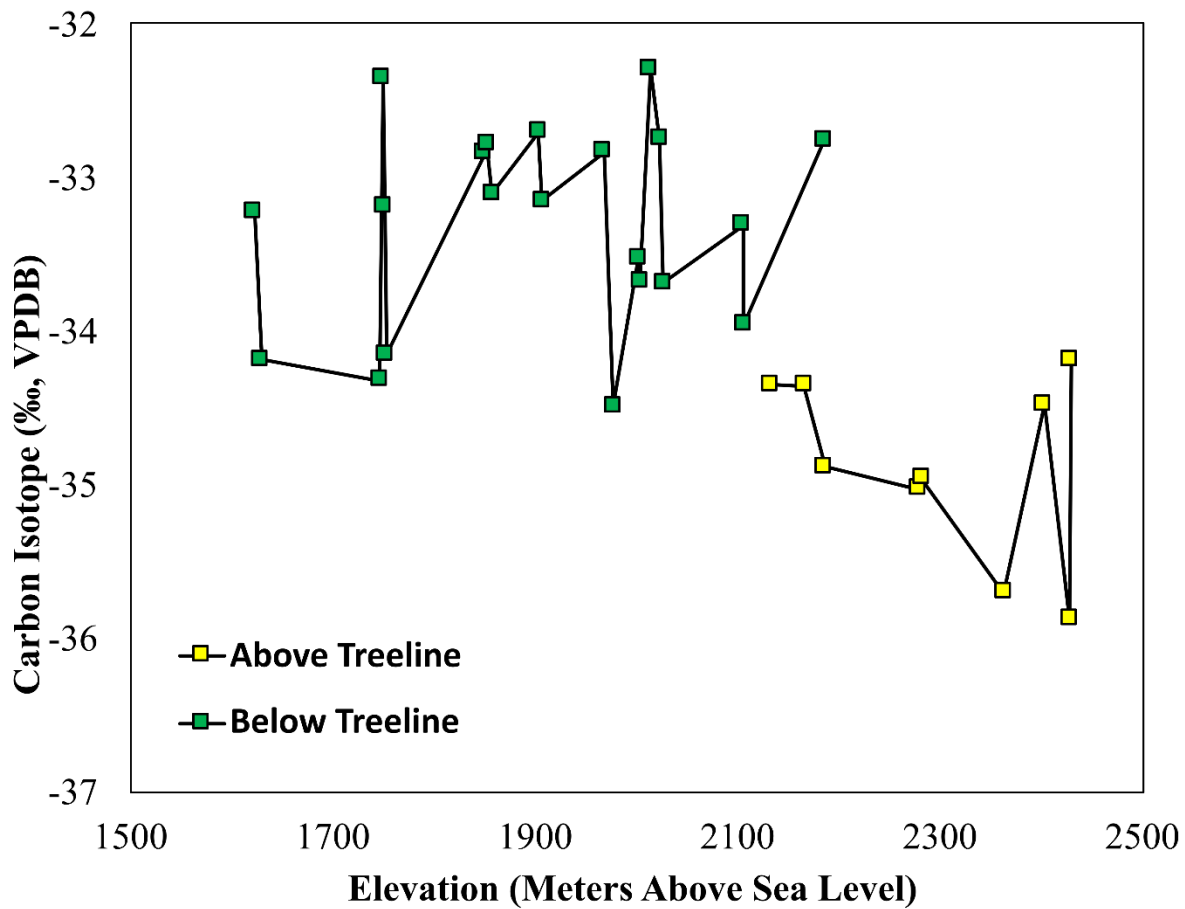
Figure 2: The  $\delta\text{D}$  and  $\delta^{13}\text{C}$  values of *n*-alkanes extracted from above treeline (green squares) and below treeline (red triangles) sediments



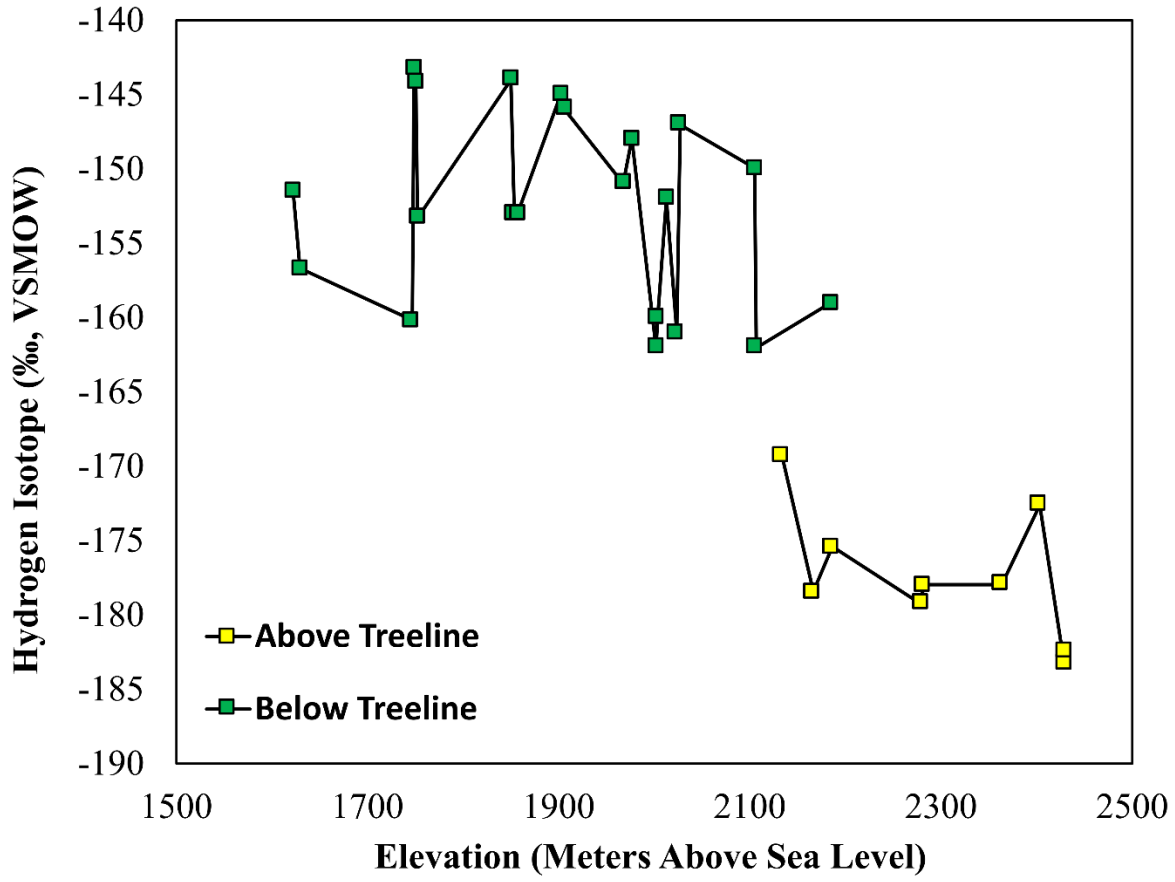
525  
526  
527  
528  
529  
530  
531  
532  
533  
534  
535  
536  
537  
538  
539  
540  
541  
542  
543  
544



545  
546



547  
548  
549  
550  
551  
552  
553  
554  
555  
556  
557  
558  
559  
560  
561  
562  
563  
564  
565  
566



567  
568  
569

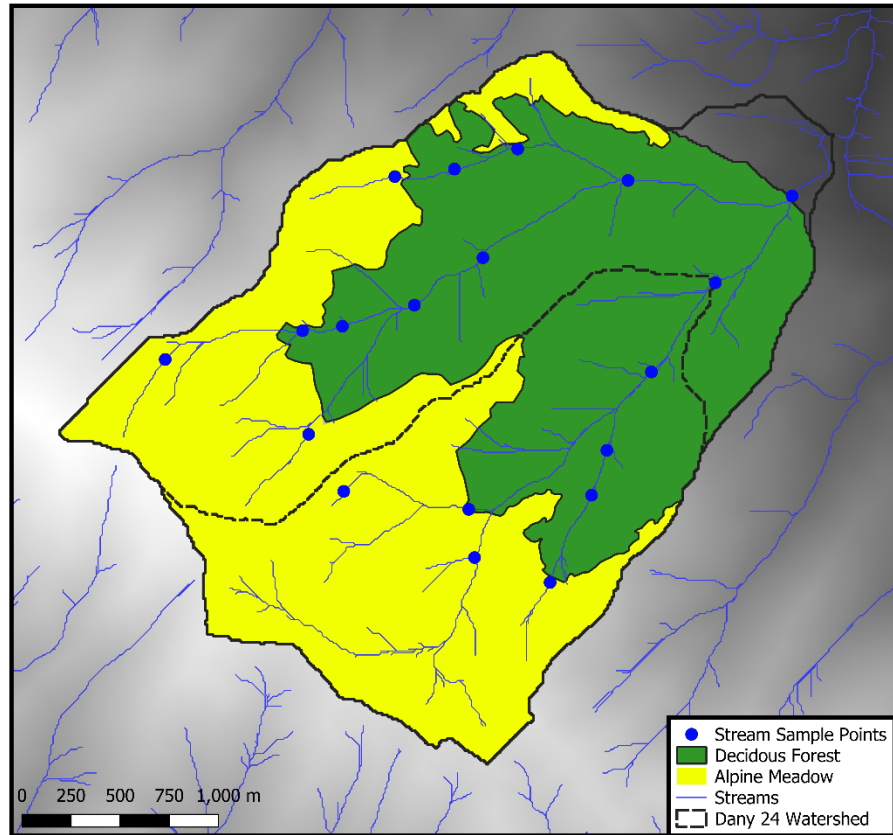


**Figure 6:** Mixing model used to calculate expected values of stream sample points. Upstream watershed area covered by deciduous forest (green) and alpine meadow (yellow) was calculated at each sample location (blue dots). Point watershed for sample 24 (dashed line) is shown here as an example.

